Electronic Supplementary Information: Direct comparison of 3-centre and 4-centre HBr elimination pathways in methyl-substituted vinyl bromides

Shubhrangshu Pandit, Balázs Hornung and Andrew J. Orr-Ewing*

School of Chemistry, University of Bristol, Cantock's Close, Bristol, BS8 1TS, UK.

S.1 Methyl migration

The premise of the current study is that 3-centre and 4-centre HBr elimination channels from methyl-substituted vinyl bromides can be selectively studied by blocking certain sites in the parent molecules using methyl groups. This premise is robust as long as the energized ground state molecules formed by internal conversion from excited states do not undergo isomerization prior to HBr elimination. It is therefore necessary to consider the possibility of methyl radical migration affecting the HBr elimination mechanisms. Calculations were performed for methyl migration within internally hot EBP-34 molecules at the same level of theory as used to identify transition states for HBr elimination. Methyl migration along the C=C bond converts internally hot EBP-34 to a carbene, 2-bromo-prop-3-ylidene. The optimized transition state energy for this methyl migration is 344 kJ mol^{-1} above the ground state of EBP-34. An RRKM calculation provided a rate coefficient of 0.35 x 10^9 s^{-1} for an EBP-34 molecule containing an excess energy corresponding to a 193-nm photon. Hence, methyl migration within EBP-34 is calculated to be ~750 times slower than the 3-centre HBr elimination and ~130 times slower than the 4-centre HBr elimination, and can be discounted in the current study. Similarly, the RRKM rate coefficient for methyl migration within BMP-3 is found to be 0.6 x 10^9 s^{-1} which is nearly one order of magnitude smaller than for 3-centre HBr elimination.
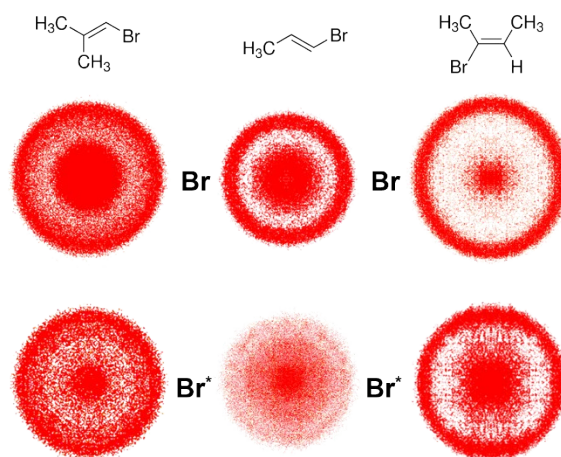
S.2 Br atom loss pathways

Fig.S.1 Velocity map images of Br ($^2P_{3/2}$) (upper row) and Br* ($^2P_{1/2}$) (lower row) fragments from 193-nm photolysis of three different bromo-alkenes, for which the structures are shown at the top of the figure. The images in the first column are from 1-Bromo-2-methyl-1-propene (BMP), the second column is for E-1-bromo-1-propene (EBP) and the third column is for E-2-bromo-2-butene (EBB).

The raw images of spin-orbit ground and excited state bromine atoms from the three bromoalkenes studied are shown in Fig. S.1. The angular distributions are isotropic because the photolysis laser was unpolarized. There are two different velocity components for both Br($^2P_{3/2}$) and Br*($^2P_{1/2}$) fragments. The fast moving fragments dominate and the observed bimodal speed distributions agree with previous reports for vinyl bromide photodissociation.[1] There are also some residual pump-laser-only background signals, with intermediate kinetic energy distributions (40-50 kJ mol^{-1}), most prominent in the Br* images from EBP. In all three cases, the signal intensity of Br was approximately 15 times larger than for Br*. In a previous study of the 193-nm photodissociation of vinyl bromide, the [Br*]/[Br] branching ratio was reported to be 0.06 ± 0.03.[1]
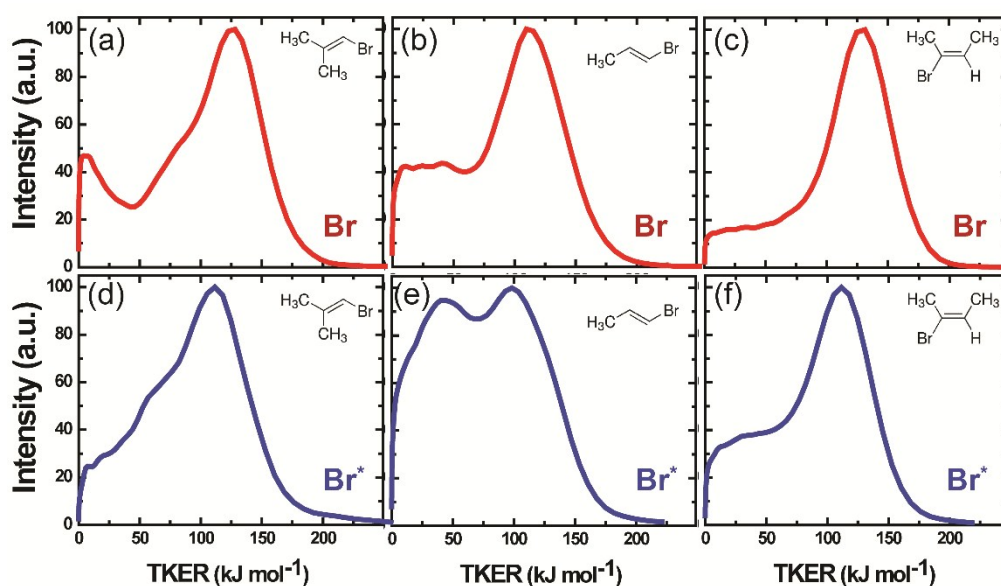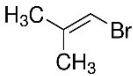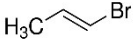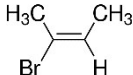
Fig. S.2 The total kinetic energy distributions of Br (upper row, (a), (b), (c)) and Br* (lower row (d), (e), (f)) and the partner methyl-substituted vinyl radicals from 193-nm photolysis of three different bromo-alkenes. TKER distributions were obtained by image analysis using a partial-slicing method. The left column ((a),(d)) is for 1-Bromo-2-methyl-1-propene (BMP), the middle column ((b),(e)) is for E-1-bromo-1-propene (EBP) and the right column((c),(f)) is for E-2-bromo-2-butene (EBB).

Fig. S.2 shows the total kinetic energy distributions for Br and Br* fragments partnering the corresponding methyl vinyl radicals from 193-nm photodissociation of BMP, EBP and EBB. Similar observations of Br/Br* fragments with high translational energies, from previous experiments on vinyl bromide,[1] were attributed to C-Br dissociation induced by a surface crossing between the $\pi_{CC}\pi_{CC}^{*}$ and the repulsive $\pi_{CC}\sigma_{CBr}^{*}$, $n_{Br}\sigma_{CBr}^{*}$ states.[1–3] The $\pi_{CC}\sigma_{CBr}^{*}$ configuration gives rise to states that lead to both spin-orbit ground and excited atomic fragments, whereas dissociation on the ground state potential energy surface (PES) only correlates to ground state Br fragments. Hence, Br* fragments form mostly by the excited state pathways.[1–3] Dissociation on a repulsive excited state favours kinetically hot Br/Br* fragments, whereas the kinetic energy distributions of Br fragments from the ground state PES peak near zero.[1]

Table S.1 Average total kinetic energies of the faster photofragments (corresponding to a bromine atom and a partner methyl-substituted vinyl radical), and the corresponding fraction of the total available energy, f_t.

Molecule	Total Kinetic Energy Distributions			
	Br($^2P_{3/2}$)		Br($^2P_{1/2}$)	
	E_{avl} = 285 kJ mol^{-1}		E_{avl} = 241 kJ mol^{-1}	
	$\langle E_t \rangle$	$f_t{}^a$	$\langle E_t \rangle$	$f_t{}^a$
H$_3$C—Br, CH$_3$	129	0.45	112	0.46
H$_3$C—Br	114	0.40	100	0.41
H$_3$C, CH$_3$, Br, H	131	0.46	111	0.46

^{a} Uncertainties lie in the range~2-3%.

Table S.1 summarizes the average total kinetic energies (for the pair of photofragments) deduced from analysis of fast Br and Br* components in the images. These TKER distributions peak 13-20 kJ mol^{-1} from one another, despite there being 44 kJ mol^{-1} of spin-orbit energy difference between Br and Br* atoms. Umemoto *et al*. observed a small difference in average total kinetic energy for the Cl and Cl* dissociation channels from chloroethenes and attributed their observations to the differences in the gradients of the repulsive PESs leading to Cl ($^{\pi}cc^{\sigma}\overset{*}{ccl}$) and Cl* ($^{n}cl^{\sigma}\overset{*}{ccl}$) near the crossing point.[4] The fraction of the total available energy that is partitioned into translational motion is similar for Br and Br* dissociation from all three molecules (see Table S.2). This observation is perhaps not consistent with different steepness of the repulsive states. Katayanagi *et al.*[1] and later Mains *et al.*[2] instead argued that the repulsive states leading to Br and Br* fragments in vinyl bromide cross the photoexcited $^{\pi}cc^{\pi}\overset{*}{cc}$ state at different points, which reduces the difference between the energies for Br and Br* channels available for translational motion.

The images also reveal slower atomic fragments with TKERs peaking near 0 kJ mol^{-1}. These components are most prominent in images from BMP photodissociation. Katayanagi *et al*. observed

similarly slow Br photofragments from vinyl bromide photolysis and assigned them to C-Br bond dissociation in the electronic ground state.[1] An alternative assignment is to Br and Br* atoms formed in coincidence with electronically excited radical co-fragments. Evidence for this behaviour has been presented for the photolysis of 2-Bromo-1-butene.[5]
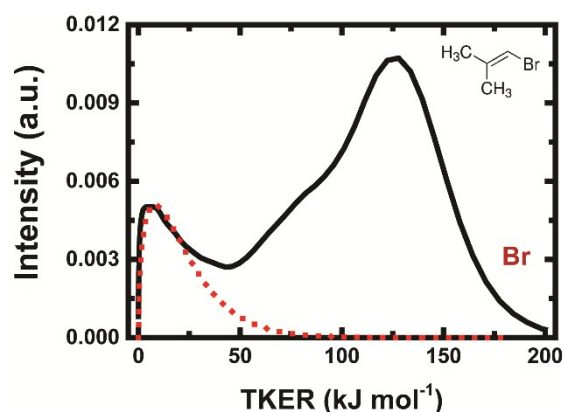

Fig. S.3 The total kinetic energy distribution of Br and its partner radical from 193-nm photolysis of BMP. The black solid line is obtained from our experiment and the red dotted line is a statistical prediction for C-Br bond dissociation in the electronic ground state. A branching ratio of 0.16 (see main text) is used to scale the amplitude of the red curve corresponding to these slower Br + vinylic radical components.

The ground state PESs of the methyl vinyl bromides correlate asymptotically with spin-orbit ground state Br atoms. This correlation accounts for the preponderance of Br over Br* photoproducts at recoil speeds associated with the ground state dissociation pathway. A calculation has been carried out to predict TKER distributions for the Br-atom dissociation pathway from the ground state, in which the translational energy distributions were modelled assuming statistical distribution of the total available energy. The faster component in the TKER distribution for Br atom and vinylic radical photofragments from BMP was fitted to two Gaussian functions and the residual (slow component) was fitted to the calculated TKER distribution (red dotted line in Fig. S.3). The second Gaussian function for the faster fragments was included to account for background pump-laser-only signals. Our calculation for Br dissociation from the electronic ground state reproduces the TKER distribution of the slower Br + vinylic radical component from BMP successfully (see Fig. S.3). This decomposition of

5

the TKER distribution indicates a branching ratio of 84 : 16 for the relative proportions of excited state and ground state C-Br bond breaking processes. These numbers are close to an earlier prediction of 86% excited state dissociation from an RRKM calculation on the photodissociation of vinyl chloride.[6] For Br* fragments, the corresponding branching ratio is estimated to be 3 ± 3 % from the integrated areas of the Gaussian fit for the fast component and the residual for the slow component. Only a very small fraction of Br dissociation takes place from the electronic ground states of EBP and EBB and therefore has not been included in the discussion.

S.3 TKER Distributions of HBr (v,J) and Organic Fragments from 193-nm EBB, BMP and EBP photolysis

S.3.1 TKER distributions from images of HBr(v=2,J) in different rotational states. Nascent HBr fragments from all three precursors were velocity map imaged state-selectively for different rotational and vibrational levels. HBr (v=2, J=0-3) and the organic co-fragments from BMP, EBP and EBB show very similar TKER distributions for all four rotational states probed (see Fig. S.4).
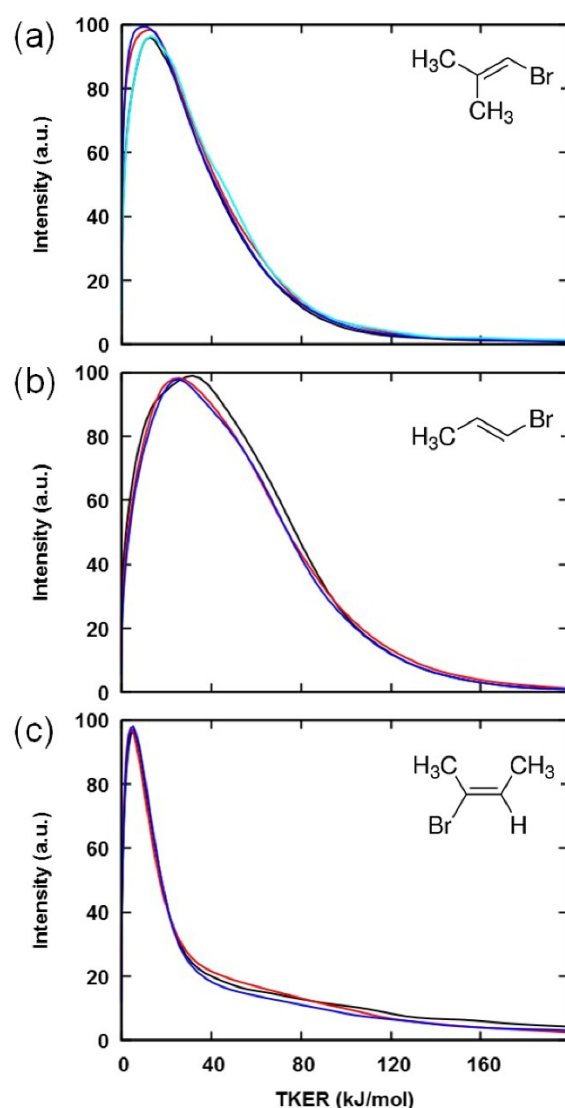

Fig. S.4 The total kinetic energy release distributions of HBr (v=2, J=0-3) and the partner organic radical fragments from all three precursors studied: (a) 1-Bromo-2-methyl-1-propene (BMP); (b) E-1-bromo-1-propene (EBP); and (c) E-2-bromo-2-butene (EBB). The red lines are for J=0, black lines are for J=1, blue lines are for J=2 and cyan lines for J=3.

S.3.2 TKER distributions deduced from images of HBr(v,J=1) in different vibrational levels v

= 0 - 2. The maximum available energy that can be transformed into total kinetic energy is ~80 kJ mol^{-1} higher when HBr is produced in its vibrational ground state v=0 compared to HBr (v=2) fragments. However, the TKER distributions are very similar irrespective of the degree of HBr vibrational excitation (see Fig. S.5).
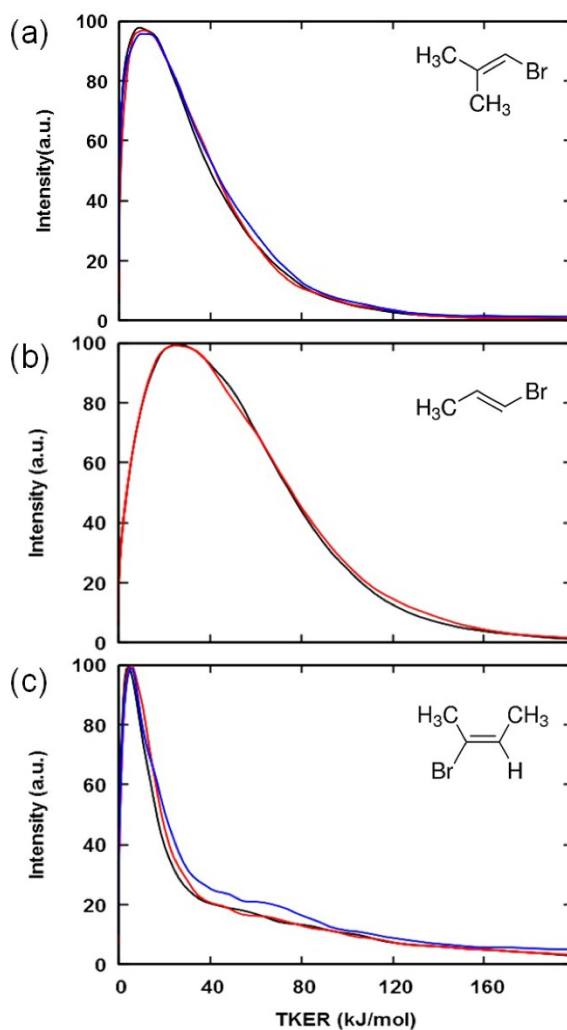

Fig. S.5 The total kinetic energy distributions of HBr (v=0-2, J=1) and its partner organic fragments from 193-nm photolysis of all three precursors: (a) 1-Bromo-2-methyl-1-propene (BMP); (b) E-1-bromo-1-propene (EBP); (c) E-2-bromo-2-butene (EBB). The red lines are for v=0, blue lines are for v=1 and black lines are for v=2.

S.4 Alternative REMPI Spectrum of HBr (v=0)

HBr(v=0) photoproducts from all three precursors were detected using the alternative (2+1) REMPI ionization scheme two-photon resonant with the $g\,^3\Sigma^+(0^+) \leftarrow X\,^1\Sigma^+$ transition, for which the REMPI efficiency is higher than that of the $F\,^1\Delta \leftarrow X\,^1\Sigma^+$ transition. This detection scheme enabled us to detect HBr(v=0) with higher rotational excitation. Fig. S.6 shows a Boltzmann plot of rotational populations of HBr (v=0) from the photodissociation of BMP. The estimated rotational temperatures (without rotational line strength correction) are 239 ± 23 K, 346 ± 28 K and 115 ± 7 K for HBr (v=0) from BMP, EBP and EBB respectively.
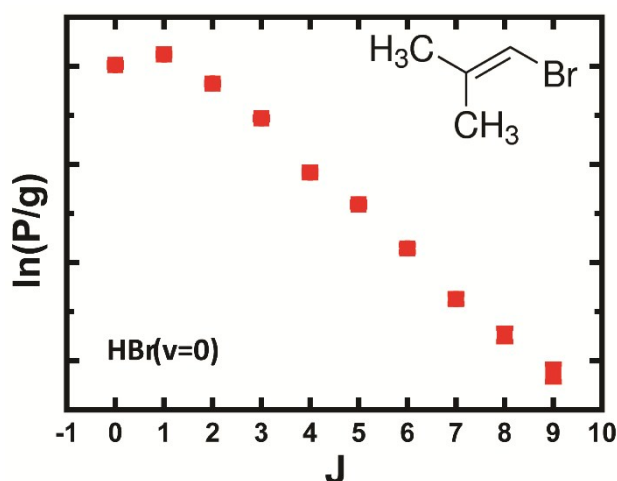

Fig. S.6 Boltzmann plot for rotational distributions of HBr(v=0) from 193-nm photolysis of BMP-3. P values are the integrated areas of individual peaks in the $g^3\Sigma^-(0^+) \leftarrow X\,^1\Sigma^+$ (2+1) REMPI spectra without any REMPI line strength correction. The degeneracy of each state is denoted by g.

References

1   H. Katayanagi, N. Yonekuira and T. Suzuki, *Chem. Phys.*, 1998, **231**, 345–353.

2   G. J. Mains, L. M. Raff and S. A. Abrash, *J. Phys. Chem.*, 1995, **99**, 3532–3539.

3   M. J. Berry, *J. Chem. Phys.*, 1974, **61**, 3114.

4   M. Umemoto, K. Seki, H. Shinohara, U. Nagashima, N. Nishi, M. Kinoshita and R.

Shimada, *J. Chem. Phys.*, 1985, **83**, 1657.

5   J. L. Miller, M. J. Krisch, L. J. Butler and J. Shu, *J. Phys. Chem. A*, 2005, **109**, 4038–4048.

6   D. A. Blank, W. Sun, A. G. Suits, Y. T. Lee, S. W. North and G. E. Hall, *J. Chem. Phys.*, 1998,

108, 5414.